Iterative correction of beam hardening artifacts in CT

Katrien Van Slambrouck, Gert Van Gompel, Michel Defrise, K. Joost Batenburg,
Jan Sijbers and Johan Nuyts
E-mail: katrien.vanslambrouck@uz.kuleuven.be

We present a method to reduce beam hardening artifacts in computed tomography. We started from the linearisation pre-correction method of Van Gompel et al. [1] and modified this model to a least squares reconstruction method, MGRA. This modification makes it more easy to interpret the physical meaning of the reconstructed values. MGRA, however, is computationally expensive and therefore, we developed an acceleration step based on a FBP density update, MFBP. All three methods have been evaluated with simulations and phantom measurements.

I. Introduction

The polychromatic nature of the X-rays in computed tomography (CT) causes beam hardening, which results in cupping and streak artifacts. Several approaches have been applied to reduce these artifacts with good results. In a first approach one uses statistical reconstruction with a polychromatic model [2], [3], [4]. The main drawback of such a model is the high computation time. Another possibility is to use a linearisation method. These methods are effective but often there are restrictions. Some methods can only be applied on a limited class of objects [5] or for limited geometries [6]. Knowledge about material properties is often required [7], [8] and also a calibration scan can be necessary [9].

Recently, Van Gompel et al. [1] and Krumm et al. [10] proposed linearisation methods for which neither spectrum nor material properties need to be known. The methods modify the measured sinogram by adding the differences of a monochromatic and a polychromatic simulation. In [1], the polychromatic sinogram is simulated using a parameterized polychromatic model that is fitted to the measured data. For the monochromatic simulation a set of monochromatic attenuation coefficients needs to be fitted based on the simulated polychromatic sinogram.

We propose a modified version of the algorithm of [1], which treats the problem as a reconstruction task rather than as a sinogram pre-correction task. For that purpose, the density in each voxel is introduced as an extra parameter set. These densities and the material characteristics are estimated from the data.

In section II the method of [1] is briefly explained and the modified model is presented. Section III describes the phantom we used to evaluate the model, the results are given in section IV. Finally in section V the results are discussed and the different algorithms are compared.

K. Van Slambrouck and J. Nuyts are with the Dept. of Nuclear Medicine, K.U.Leuven, Leuven, Belgium. G. Van Gompel is with the Dept. of Radiology, UZ Brussel, Brussels, Belgium. M. Defrise is with the Dept. of Nuclear Medicine, V.U.Brussel, Brussel, Belgium. K.J. Batenburg and J. Sijbers are with the VisionLab, U. Antwerp, Antwerp, Belgium

This work was financially supported by the SBO-project QUANTIVIAM (060819) of the Institute for the Promotion of Innovation through Science and Technology in Flanders (IWT-Vlaanderen).

II. Models

The original model and the newly proposed algorithms are all based on the hypothesis that there are N different materials present in the object with $n = 1, ..., N$ and that each voxel can only contain one material defined by a binary variable $s_{n,j}$ taking the value $s_{n,j} = 1$ if voxel j contains n and $s_{n,j} = 0$ otherwise.

A. Sinogram pre-correction method (GVG)

In the model of [1] the measured intensity I_p^{meas} is approximated by

$$I_p^{\text{sim}}(i) = I_0 \sum_{e=1}^{E} I_e^F \exp\left(- \sum_{n=1}^{N} \mu_{n,e} \sum_j l_{ij} s_{n,j} \right) \quad (1)$$

where i denotes the projection ray, E is the number of energy bins that will be used to simulate the spectrum, l_{ij} is the intersection length of ray i with pixel j and $I_e^F = I_e / I_0$ is the fraction of the total spectrum corresponding to energy bin e, with $I_0 = \sum_e I_e$, the

intensity in absence of the object. The polychromatic attenuation, estimated from the parameters $\{\boldsymbol{\mu}, \boldsymbol{I}^F, \boldsymbol{s}\}$ for ray i is then given by $A_p^{\text{sim}}(i) = \ln\left(\frac{I_0(i)}{I_p^{\text{sim}}(i)}\right)$. The corresponding estimate from the measurement is $A_p^{\text{meas}}(i) = \ln\left(\frac{I_0(i)}{I_p^{\text{meas}}(i)})\right)$.

The measurement is corrected by iteratively adding the difference between the simulated monochromatic and polychromatic attenuation:

$$A_m^{\text{cor},w}(i) = A_p^{\text{meas}}(i) + \left(A_m^{\text{sim},w}(i) - A_p^{\text{sim},w}(i)\right) \quad (2)$$

where w is the iteration number and $A_m^{\text{cor},0} = A_p^{\text{meas}}$. The monochromatic simulation is given by

$$A_m^{\text{sim}}(i) = \sum_{n=1}^{N} \mu_n^{\text{ref}} \sum_j l_{ij} s_{n,j}$$

with μ_n^{ref}, the reference attenuation coefficient for material n. In each iteration, $A_m^{\text{cor},w}$ is reconstructed with filtered backprojection (FBP), and segmented with thresholding to produce a new estimate of $\boldsymbol{s}$. Then $\boldsymbol{\mu}$, $\boldsymbol{I}^F$ and $\boldsymbol{\mu}^{\text{ref}}$ are estimated by minimizing (3) and (4).

$$\Phi(\boldsymbol{\mu}, \boldsymbol{I}^F, \boldsymbol{s}) = \sum_i \left(\ln\left(\frac{I_p^{\text{meas}}(i)}{I_0(i)}\right) - \ln\left(\sum_{e=1}^{E} I_e^F \exp\left(-\sum_{n=1}^{N} \mu_{n,e} \sum_j l_{ij} s_{n,j}\right)\right)\right)^2 \quad (3)$$

$$\begin{aligned}\Psi(\boldsymbol{\mu}, \boldsymbol{s}) &= \sum_i \left(A_m^{\text{sim}}(i) - A_p^{\text{sim}}(i)\right)^2 \\ &= \sum_i \left(\sum_{n=1}^{N} \mu_n^{\text{ref}} \sum_j l_{ij} s_{n,j} \right. \\ &\quad \left. - \ln\left(\sum_{e=1}^{E} I_e^F \exp\left(-\sum_{n=1}^{N} \mu_{n,e} \sum_j l_{ij} s_{n,j}\right)\right)\right)^2\end{aligned} \quad (4)$$

In [1] this method was applied on piecewise uniform objects with three materials. It was found that the use of three energy bins is sufficient to make an appropriate reconstruction. We will refer to this model as the GVG model.

B. Modified model (MFBP and MGRA)

The major difference between the modified model and GVG is that a density d_j is assigned to each voxel in addition to the material index $s_{n,j}$ so that the cost function (3) becomes:

$$\tilde{\Phi}(\boldsymbol{\mu}, \boldsymbol{I}^F, \boldsymbol{d}, \boldsymbol{s}) = \sum_i \left(\ln\left(\frac{I_p^{\text{meas}}(i)}{I_0(i)}\right) - \ln\left(\sum_{e=1}^{E} I_e^F \exp\left(-\sum_{n=1}^{N} \mu_{n,e} \sum_j l_{ij} d_j s_{n,j}\right)\right)\right)^2 \quad (5)$$

where d_j denotes the density in pixel j. To minimize this cost function we need to estimate the attenuation coefficients $\boldsymbol{\mu}$, the fractional energies $\boldsymbol{I}^F$, the density $\boldsymbol{d}$ and the segmentation $\boldsymbol{s}$. Based on the estimated parameters we produce the following image for visual inspection:

$$R_w = d^w \sum_n \mu_n^{\text{mono},w} s_n^w \quad (6)$$

where $\boldsymbol{\mu}^{\text{mono}}$ are monochromatic attenuation coefficients which can be estimated by $\boldsymbol{\mu}^{\text{ref}}$ as in GVG, but also the mean attenuation can be chosen. For an easy comparison we choose $\boldsymbol{\mu}^{\text{ref}}$. All parameters are iteratively updated.

Algorithm

Each iteration of the modified algorithms consists of the following steps:

1) Segmentation: The current image estimate R_w is segmented to update the material indices $s_{n,j}$. This is accomplished by a threshold method. The thresholds are adapted in such a way that the new thresholds lower the cost function (5). This is done by a gradient descent algorithm.

2) Density: As a second step we update the density. Two approaches for the density step are proposed. The first one uses a gradient descent step ensuring that $\tilde{\Phi}(\boldsymbol{\mu}, \boldsymbol{I}^F, \boldsymbol{d}, \boldsymbol{s})$ does not increase. The second one is inspired by the iterative filtered-backprojection method. A new image is obtained as $R_w^{'} = R_w + \text{FBP}(A_p^{\text{meas}} - A_p^{\text{sim}})$ and the updated densities are then directly obtained by setting

$$R_w^{'} = d^{w+1} \sum_{n=1}^{N} \mu_n^{\text{mono},w} s_n^{w+1}.$$

In the following text the modified model with FBP density update will be called the MFBP model. In case a gradient descent update is used we will call it the MGRA model. The gradient descent update contains a projection and backprojection, and can be accelerated with ordered subsets.

3) Attenuation and fractional energy: Updated attenuation coefficients and fractional energies are calculated by a gradient based minimization of the cost function (5) with constant density and constant segmentation.

4) Visualization: After estimation of the parameters, we calculate the monochromatic attenuation coefficients and update the visualization (6).

In the first iteration we segment the uncorrected FBP reconstruction, $\mathrm{FBP}(A_p^{\mathrm{meas}})$, and we assume the density to be equal to one everywhere. As was done in [1], we chose to use three energy bins and we accelerated the method by using a downsampled sinogram together with a Gaussian filter till the following stop condition is met:

$$\frac{\tilde{\Phi}^{w-1} + \tilde{\Phi}^{w}}{\tilde{\Phi}^{w-3} + \tilde{\Phi}^{w-2}} > 0.9. \tag{7}$$

Secondly, we iterate again till stop condition (7) but without a filter. Finally, we upsample the result and do two full size iterations.

III. Materials

We tested this new model on simulations and on a phantom measurement. Here, only the phantom measurements will be presented. The *bean phantom* (3cm x 1cm) is depicted in figure 1(a). It consists of four materials: air, plexiglass, white spirit, and water. The density of water is only slightly higher than the density of plexiglass, the main material, whereas the density of white spirit is substantially lower. The algorithms were applied with $N = 3$, consequently, the water part will not be segmented separately for this phantom.

A Skyscan 1172 μCT at 60 kV was used to obtain the data. Hardware filtering and the beam hardening correction option were turned off. The central slice of the cone beam geometry was rebinned to a parallel beam geometry. The parallel beam sinogram consists of 300 views, equally spaced with an angular range $[0, \pi[$ and 1000 radial samples. We used downsampling factor 4 for the radial samples and 2 for the views. The Gaussian filter had a standard deviation of 1.5 pixels. FBP reconstruction is done using a Hamming filter with cutoff frequency 0.5.

IV. Results

Three algorithms are compared: the original GVG pre-correction model, and the two proposed reconstruction algorithms: the modified model with FBP density update (MFBP) and the modified model with the gradient density update (MGRA).

Figure 1 shows the uncorrected FBP reconstruction of the bean phantom and the results obtained with GVG, MFBP and MGRA. The evolution of the cost function $\tilde{\Phi}(\boldsymbol{\mu}, \boldsymbol{I}^F, \boldsymbol{d}, \boldsymbol{s})$ (5) as a function of the iteration number is shown in figure 2.

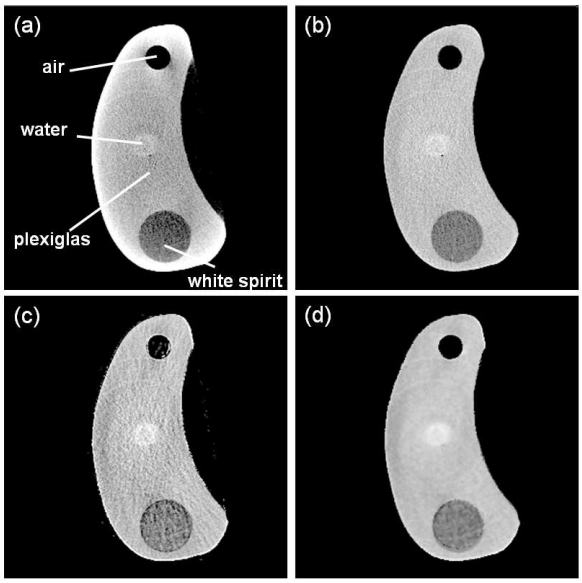

Fig. 1. **Bean phantom**. Uncorrected FBP reconstruction (a), correction with GVG (b), correction with MFBP (c) and correction with MGRA (d).

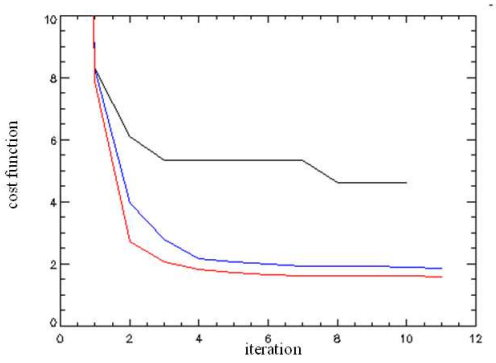

Fig. 2. Evolution of the cost function $\tilde{\Phi}(\boldsymbol{\mu}, \boldsymbol{I}^F, \boldsymbol{d}, \boldsymbol{s})$ as a function of the iteration number. GVG: black line, MFBP: blue line and MGRA: red line.

V. Discussion

The GVG pre-correction method is fast and effective. However, it is difficult to assign a physical meaning to the reconstructed values. Therefore, we proposed two related iterative reconstruction algorithms. The algorithms are based on an extension of the original cost function $\Phi(\boldsymbol{\mu}, \boldsymbol{I}^F, \boldsymbol{s})$ (4) to $\tilde{\Phi}(\boldsymbol{\mu}, \boldsymbol{I}^F, \boldsymbol{d}, \boldsymbol{s})$ (5). The main difference between both is the introduction of a material density, which explicitly models the deviation from the segmented image. In the original method, this deviation is incorporated

in an implicit way, by reconstructing the sum of the measured sinogram and a correction term deduced from the segmentation. In the MGRA method, each operation in the iteration attempts to decrease the cost function, and is guaranteed not to increase it. A monotonic decrease with effective convergence was observed in all simulations. Unfortunately, the cost function is not convex, and convergence to the global maximum is not guaranteed.

For GVG and MFBP, the cost function does not decrease systematically at every iteration, but effective convergence was still observed. The value of the cost function obtained with the reconstruction methods (MGRA and MFBP) is usually lower than the one obtained with the GVG method. It is difficult to compare the corresponding reconstructions for two reasons. First, the meaning of the reconstructed values is not the same in the pre-correction and the reconstruction methods. Second, the different algorithms seem to converge to a local minimum as intended, but the local minimum may be different. The difference in image quality is then due to the anecdotal (image dependent) convergence trajectory and not to fundamental differences between the methods. As illustrated in figure 1, all three methods give similar results.

MGRA has the best theoretical foundation but it is significantly slower than GVG and MFBP and hence cannot be used in daily practice. Especially the density update step takes a lot of computation time. Therefore, we introduced the faster FBP update step in MFBP. This change results in a strong acceleration. Monotonic decrease of the cost function $\tilde{\Phi}(\boldsymbol{\mu}, \boldsymbol{I}^F, \boldsymbol{d}, \boldsymbol{s})$ is no longer guaranteed, but good results were obtained in simulations and the first experiment on real data (figure 2). However, the MFBP correction method is more sensitive to noise compared to GVG and MGRA.

Originally, Otsu [11] thresholding was used for the segmentation in the GVG method. However, this approach did not always produce a decrease of the cost function. Here, the thresholds were determined by minimizing the cost function, which improved the convergence behavior. The disadvantage of this method is the need to calculate several projections while updating the segmentation. This is a time consuming job and often the changes to the segmentation are small. This step could be strongly accelerated, by using a projector that only projects the differences between the old and new segmentations, as was done in [12].

VI. Conclusion

The advantages of the modified algorithm are:

- The problem is defined as an explicit optimization problem, which makes it easier to interpret and analyze the reconstructed image. The reconstructed values correspond to the parameters of an (approximate) model, whereas in the original method, it is more difficult to assign a physical meaning to the reconstructed image values.
- The introduction of the density offers the possibility to use this method for objects with materials which have small density differences. This way, this important feature of the method of [1] could be preserved.

The limitations of the proposed algorithm are

- The modified model MGRA needs more computation time, while the results are not very different from those of the original algorithm.
- The MGRA method is too slow for routine use. However, it is useful as a reference method when evaluating the performance of the two related approximation methods.

References

[1] Van Gompel G., PhD thesis: *Towards accurate image reconstruction from truncated X-ray CT projections*, Antwerp 2009.

[2] B. De Man, J. Nuyts, P. Dupont, G. Marchal, P. Suetens."An iterative maximum-likelihood polychromatic algorithm for CT." *IEEE Trans Med Imaging*, 2001; 20 (10): 999-1008.

[3] I. Elbakri and A. Fessler. "Statistical Image Reconstruction for Polyenergetic X-Ray Computed Tomography." *IEEE Transactions on Medical Imaging*; 2002, 21 (2):89-99.

[4] N. Menvielle, Y. Goussard, D. Orban, G. Soulez. "Reduction of beam-hardening artifacts in X-ray CT." *Proceedings of the 2005 IEEE Engineering in Medicine and Biology 27th Annual Conference Shanghai*, China, September 1-4, 2005

[5] H. Goa, L. Zhang, Z. Chen, Y. Xing and L.Shuanglei. "Beam hardening correction for middle-energy industrial computerized tomography." *IEEE Transactions on Nuclear Science*; 2006, 53 (5):2796-2807.

[6] X. Mou, S. Tang and H. Yu. "Comparison on beam hardening correction of CT based on HL consistency and normal water phantom experiment." *SPIE medical Imaging*; 2006: 6318V

[7] V. Vedula and P. Munshi. "An improved algorithm for beam hardening corrections in experimantal X-ray tomography." *NDT&E International*; 2008, 41: 25-31.

[8] Y. Censor, T. Elfving and G.T. Herman. "A method of iterative data refinement and its applications." *Math. Meth. in the Appl. Sci.*; 1985, 7:108-123.

[9] R. Grimmer, C. Maass, M. Kachelreiss. "A new method for cupping and scatter precorrection for flat detector CT." *IEEE Nuclear Science SYmp. Conf. Rec.*; 2009: 3517-3522.

[10] M. Krumm , S. Kasperk and M. Franz. "Reducing nonlinear artifacts of multi-material objects in industrialised 3D computed tomography." *NDT&E International*; 2008, 41: 242-251.

[11] N. Otsu. "A threshold selection mehtod from gray-level histograms." *Trans. on Systems, Man, and Cybernetics*; 1979, 5 (9): 62-66.

[12] K. J. Batenburg and J. Sijbers. "Optimal threshold selection for tomogram segmentation by projection distance minimization." *IEEE Trans. Medical Imaging*; 2009, 28 (5):676-686.